Kinetics of the *E. Coli* Replication Factor DnaC Protein−Nucleotide Interactions. II. Fluorescence Anisotropy and Transient, Dynamic Quenching Stopped-Flow Studies of the Reaction Intermediates†

Roberto Galletto and Wlodzimierz Bujalowski*

Department of Human Biological Chemistry & Genetics and The Sealy Center for Structural Biology, The University of Texas Medical Branch at Galveston, Galveston, Texas 77555-1053

Received February 12, 2002; Revised Manuscript Received April 8, 2002

ABSTRACT: The nature of the intermediates in the binding of MANT-ATP and MANT-ADP to the *E. coli* replicative factor DnaC protein (accompanying paper) has been examined using the fluorescence intensity, anisotropy, and transient dynamic quenching stopped-flow techniques. Using molar fluorescence intensities of individual intermediates of the reaction, we derived the Stern−Volmer equation that provides a direct method to quantitatively address the quenching of the fluorescence of a transient intermediate by an external, neutral quencher. The data indicate that in the first intermediate, $(C)_1$, the solvent has full access to the MANT group. Thus, the nucleotide-binding site is located on the surface of the protein, fully open to the solvent. Moreover, formation of the first intermediate does not affect the structure of the binding site. On the other hand, in the second intermediate, $(C)_2$, the entire binding site changes its conformation, resulting in diminished access of the solvent to the bound nucleotide. The time course of the fluorescence anisotropy in the reaction provides direct, unique insight into the mobility of bound nucleotides in each intermediate. The analysis is facilitated by the fact that the anisotropy can be expressed as a function of the relative molar intensities and steady-state anisotropies of the individual intermediates. The major decrease of the nucleotide mobility occurs in the formation of the first intermediate and reflects the fact that the MANT group is immobilized to a similar extent as the ribose region of the bound nucleotides. Transition to the second intermediate and closing of the binding site leads to only a moderate, additional decrease of nucleotide mobility. The temperature effect on the studied interactions indicates that the formation of individual intermediates is accompanied by very different enthalpy and entropy changes predominantly generated from the structural changes of the protein. Analysis of the salt effect indicates that the net release of a single ion, observed in equilibrium studies, occurs in the formation of the first intermediate. The lack of any salt effect on the $(C)_1 \leftrightarrow (C)_2$ transition indicates that the closing of the binding site does not include a net ion release or uptake. Moreover, prior to the nucleotide binding, the conformational transition of the DnaC protein is exclusively controlled by the nucleotide binding and release.

The DnaC protein is an essential replication factor in the *Escherichia coli* cell involved in initiation and elongation stages of the DNA replication (*1*−*6*, accompanying paper). Both, the formation of the replication fork and the assembly of the primosome absolutely require the presence of the DnaC protein (*1*, *7*, *8*). Current views on the role of the DnaC protein in DNA replication strictly relate it to the highly specific interactions of the protein with the *E. coli* primary replicative helicase, the DnaB protein (*1*−*5*, *7*−*10*). These crucial protein−protein interactions are thought to be under specific ATP control. However, even on qualitative level, the mechanism by which the ATP binding controls the DnaC-DnaB interactions is not understood.

It has been proposed that, in contrast to ATP, ADP does not support the DnaC−DnaB interactions (*1*, *7*, *8*). Because the DnaC protein does not have intrinsic ATPase activity, the hydrolysis of the cofactor bound to the helicase seems to play role in controlling the DnaC binding and release, although this has never been proven. The lack of intrinsic ATPase activity leads to the natural conclusion that binding of ATP, but not ADP, induces conformational changes in the DnaC protein and the increasing protein affinity for the helicase (*7*, *8*).

The energetics of the DnaC protein interactions with the nucleotide cofactors have been recently reported by us (*11*). The protein has a single nucleotide-binding site that is highly specific for the adenine base. The most surprising result is that both ATP and ADP have the same affinity for the nucleotide-binding site of the DnaC protein (*11*). Thus, specific and efficient association of the nucleotides with the DnaC protein is not enough to trigger specific conformational changes of the protein that lead to an increased affinity toward the DnaB helicase. Fluorescence stopped-flow studies of the dynamics of the binding of ATP and ADP fluorescent analogues, MANT-ATP and MANT-ADP, to the DnaC protein are described in the accompanying paper. The

† This work was supported by NIH Grants GM-46679 (to W. B.).

* Corresponding author. Tel: (409) 772-5643. Fax: (409) 772-1790. E-mail: wbujalow@utmb.edu.

[1] Abbreviations: MANT-ATP, 3′-O-(*N*-methylantraniloyl)-5′-triphosphate; MANT-ADP, 3′-O-(*N*-methylantraniloyl)-5′-diphosphate; Tris, tris(hydroxymethyl)aminomethane; DTT, dithiothreitol.

10.1021/bi020127w CCC: $22.00
Published on Web 06/19/2002

obtained data indicate that prior to the nucleotide binding, the DnaC protein exists in the equilibrium between the two conformational states. The intrinsic binding of the nucleotide to one of the protein conformations is a two-step, sequential reaction leading to the formation of two protein−nucleotide intermediates, $(C)_1$ and $(C)_2$ (accompanying paper). Both MANT-ATP and MANT-ADP bind to the same protein conformation. The protein-nucleotide intermediates differ significantly in the physical environment surrounding the ribose region of the bound nucleotide.

Fundamental aspects of nucleotide interactions with the DnaC protein are still not well understood, thus hindering the understanding of the activities of this essential replication factor. In this communication, we quantitatively examine the nature of the intermediates in the nucleotide binding to the DnaC protein. We derived a Stern−Volmer equation that provides a general and direct way to quantitatively address the fluorescence quenching of the transient intermediate by an external, neutral quencher. The obtained data indicate that, in the $(C)_1$ intermediate, the nucleotide-binding site is located on the surface of the protein and is open to the solvent. In the second intermediate, $(C)_2$, the entire binding site changes its conformation, resulting in diminished access of the solvent to the bound nucleotide. The time course of the fluorescence anisotropy in the relaxation process provides evidence that the major decrease of the nucleotide mobility occurs in the formation of $(C)_1$. Thermodynamic analysis indicates that enthalpy and entropy changes, accompanying the formation of different intermediates, are predominantly generated by structural changes of the protein. The kinetic studies of the salt effect indicate that a single ion is released in the formation of $(C)_1$. The following $(C)_1 \leftrightarrow (C)_2$ transition, i.e., closing of the binding site, does not include net ion release or uptake. Moreover, prior to the nucleotide binding, the salt in solution does not affect the conformational transition of the DnaC protein.

MATERIALS AND METHODS

Reagents and Buffers. All chemicals were reagent grade. All solutions were made with distilled and deionized 18 MΩ (Milli-Q) water. The standard buffer, T4, is 50 mM Tris adjusted to pH 8.1 at appropriate temperatures with HCl, 5 mM $MgCl_2$, 10% glycerol, and 1 mM DTT. The salt concentration in the buffer is included in the text.

Nucleotides. MANT-ATP and MANT-ADP were synthesized as described (*12*−*16*). The concentrations of the nucleotides were spectrophotometrically determined using the extinction coefficient $\epsilon_{356} = 5800\ M^{-1}\ cm^{-1}$.

DnaC Protein. The *E. coli* DnaC protein was purified as previously described by us (*11*). The concentration of the protein was spectrophotometrically determined using the extinction coefficient $\epsilon_{280} = 23.2 \times 10^4\ M^{-1}\ cm^{-1}$ (*11*).

Stopped-Flow Kinetics. All fluorescence stopped-flow kinetic experiments were performed using the SX.18MV stopped-flow instrument (Applied Photophysics, Leatherhead, UK) equipped with the FP.1 fluorescence polarization/anisotropy accessory, as described in the accompanying paper. The relaxation times and amplitudes for each kinetic trace were determined using the nonlinear, least-squares software provided by the manufacturer, with the exponential function defined as

$$F(t) = F(\infty) + \sum_{i=1}^{n} A_i \exp(-\lambda_i t) \quad (1)$$

where $F(t)$ is the total fluorescence intensity at time t, $F(\infty)$ is the total fluorescence intensity at time $t = \infty$, A_i is the amplitude corresponding to the ith relaxation process, λ_i is the time constant (reciprocal relaxation time) characterizing the ith relaxation process, and n is the number of relaxation processes. All further analyses of the data were performed using Mathematica (Wolfram, Urbana,IL) and KaleidaGraph (Synergy Software, PA) on MacIntosh G4 computer.

RESULTS

Kinetics of MANT-ATP and MANT-ADP Binding to the DnaC Protein in the Presence of Acrylamide. Kinetic data described in the accompanying paper indicate that binding of MANT-ATP and MANT-ADP to the DnaC protein proceeds through the mechanism

$$(DnaC)_1 \underset{k_{-1}}{\overset{k_1}{\rightleftarrows}} (DnaC)_2$$

$$N + (DnaC)_2 \underset{k_{-2}}{\overset{k_2}{\rightleftarrows}} (C)_1 \underset{k_{-3}}{\overset{k_3}{\rightleftarrows}} (C)_2 \quad (2)$$

Thus, the protein exists in two conformational states, and the nucleotide cofactors bind to one of the protein conformations in a two-step, sequential reaction. Molar relative fluorescence intensities F_2 and F_3 characterizing the two intermediates $(C)_1$ and $(C)_2$, obtained through quantitative amplitude analyses, provided the first indication that $(C)_1$ and $(C)_2$ differ in the physical environment around the MANT moiety. To obtain additional information about the nature of the formed intermediates, we performed stopped-flow fluorescence studies of the binding of both MANT-ATP and MANT-ADP to the DnaC protein in the presence of acrylamide, an efficient, dynamic quencher of the MANT group fluorescence (*14*, *15*). Although acrylamide is a neutral molecule with very weak, if any, binding affinity for proteins, the experiments have been carried out in a limited range of the quencher concentration in order to avoid any profound effect of the quencher on the observed rate parameters (*17*).

Kinetic experiments of the MANT-ATP binding to the DnaC protein have been performed under pseudo-first-order conditions with respect to the nucleotide concentration. The stopped-flow trace of the MANT-ATP fluorescence, after mixing 2×10^{-6} M DnaC protein with 2.8×10^{-5} M nucleotide (final concentration) in buffer T4 (pH 8.1, 20 °C) containing100 mM NaCl and 20 mM acrylamide, is shown in Figure 1. The concentration of acrylamide is constant before and after the mixing. The kinetic traces have been collected in two time bases, 0.5 and 100 s. The continuous line in Figure 1 is a nonlinear, least-squares fit of eq 1 to the experimental kinetic trace, using a three-exponential fit (accompanying paper). As indicated by the dashed line in Figure 1 and included residuals, using a two- exponential fit does not properly represent the experimental data (accompanying paper).

The reciprocal relaxation times $1/\tau_1$, $1/\tau_2$, and $1/\tau_3$, characterizing the three binding steps as a function of the total MANT-ATP concentration, are shown in Figure 2a−c. The largest reciprocal time, $1/\tau_1$, shows linear dependence

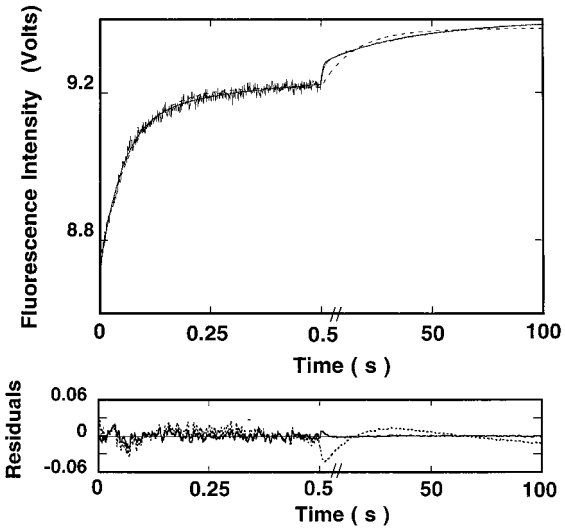

FIGURE 1: Fluorescence stopped-flow kinetic trace ($\lambda_{ex} = 356$ nm, $\lambda_{em} > 450$ nm) recorded in two time bases, 0.5 and 100 s, after mixing the DnaC with MANT-ATP in buffer T4 (pH 8.1, 20 °C) containing 100 mM NaCl and 20 mM acrylamide. The final concentrations of the DnaC and the nucleotide are 2×10^{-6} and 2.8×10^{-5} M, respectively. The solid line is the three-exponential nonlinear, least-squares fit of the experimental curve using eq 1. The dashed line is the two-exponential nonlinear, least-squares fit of the experimental curve using eq 1. The lower panel shows the residuals of the fit using the two-exponential (---) and three-exponential (—) functions, respectively.

upon [MANT-ATP]. The reciprocal relaxation times, $1/\tau_2$ and $1/\tau_3$, show independence of [MANT-ATP] in the examined range of the nucleotide concentration. The dependence of the relative individual amplitudes A_1, A_2, and A_3 for the three relaxation steps upon the logarithm of the total MANT-ATP concentration is shown in Figure 3. The behavior of both relaxation times and amplitudes is, within experimental accuracy, the same as that observed in the absence of the quencher (accompanying paper). Thus, the presence of acrylamide does not change the behavior of the observed relaxation process and has little effect on the rate parameters of the reaction. The analyses of the relaxation data have been performed using the matrix projection operator method, as described in the accompanying paper. Analogous experiments have been performed at different acrylamide concentrations and the obtained data are included in Table 1.

Inspection of the results in Table 1 shows that the behavior of the relative molar fluorescence intensities F_2 and F_3, characterizing the $(C)_1$ and $(C)_2$ intermediates, is different in response to the presence of the increasing quencher concentration in solution. In the absence of the quencher, the value of $F_2 = 2.40 \pm 0.11$ is unaffected by the increasing concentration of acrylamide. On the other hand, the value of $F_3 = 8.64 \pm 0.21$ increases with the increased [acrylamide] reaching the value of 9.91 ± 0.20 at 50 mM acrylamide, the highest applied concentration of the quencher (Table 1). Such diametrically different behavior of both relative molar fluorescence intensities provides strong evidence that the exposure of the MANT group to the solvent in both intermediates is significantly different.

Transient, Dynamic Fluorescence Quenching Studies of Individual Intermediates for the MANT-ATP Binding to the DnaC Protein. Stern−Volmer Quenching Constant for

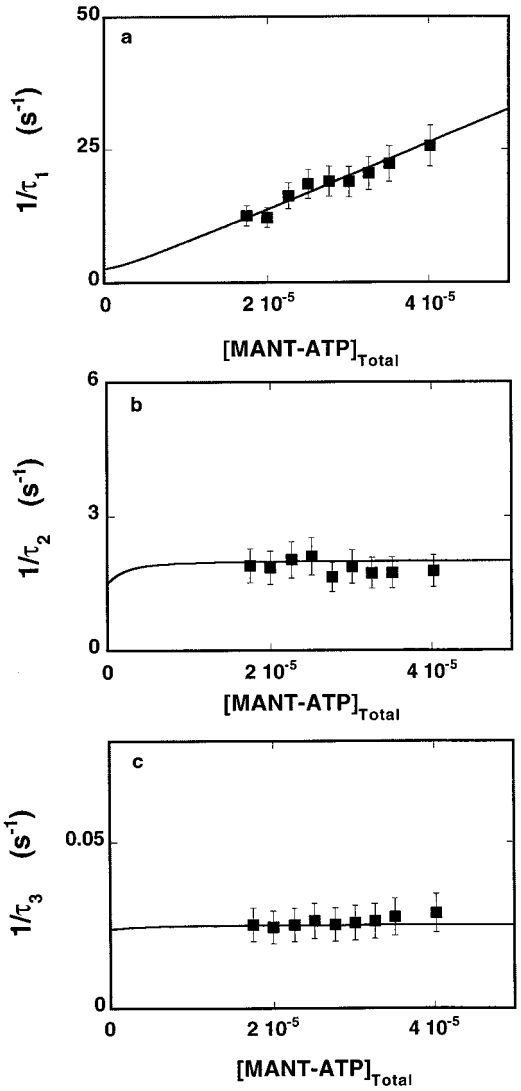

FIGURE 2: Dependence of the reciprocal of the relaxation times for the binding of MANT-ATP to the DnaC protein in buffer T4 (pH 8.1, 20 °C), containing 100 mM NaCl and 20 mM acrylamide, upon the total concentration of the nucleotide. The solid lines are nonlinear, least-squares fits of the experimental data to the mechanism, defined by eq 2, using rate constants $k_1 = 2$ s^{-1}, $k_{-1} = 0.61$ s^{-1}, $k_2 = 6.3 \times 10^5$ M^{-1} s^{-1}, $k_{-2} = 1.5$ s^{-1}, $k_3 = 0.0012$ s^{-1}, and $k_{-3} = 0.024$ s^{-1} (Table 1). (a) $1/\tau_1$, (b) $1/\tau_2$, and (c) $1/\tau_3$. The error bars are standard deviations obtained from 3−4 independent experiments.

Individual Intermediates of the Reaction. Quantitative analysis of the dynamic quenching process requires determination of the Stern−Volmer quenching constant (*17*−*19*). We previously described both theoretical and experimental aspects of the steady-state dynamic quenching analysis of the free and bound fluorescing ligand to a macromolecule (*19*). Here, we provide a quantitative description of the method, as applied to the individual transient intermediates of a reaction.

The quenching of the fluorescence emission by an external collisional quencher is conveniently described by the Stern−Volmer equation as (*17*−*19*)

$$\frac{F_L^o}{F_L^q} = 1 + k_q\tau_o[Q] = 1 + K_{SV}{}^o[Q] \qquad (3)$$

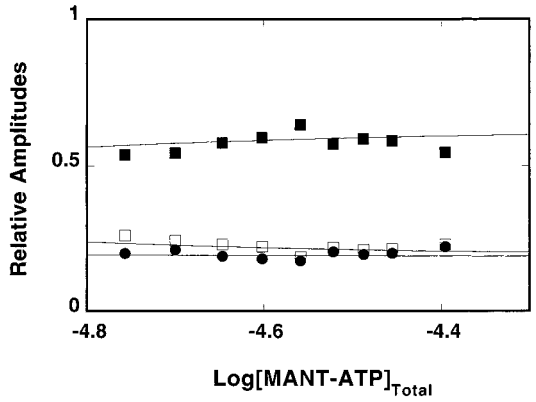

FIGURE 3: Dependence of the individual relaxation amplitudes of the kinetic process of MANT-ATP binding to the DnaC protein in buffer T4 (pH 8.1, 20 °C), containing 100 mM NaCl and 20 mM acrylamide, upon the logarithm of the total concentration of the ATP analogue. The solid lines are computer fits according to the mechanism defined by eq 2, using eq A8 (accompanying paper, Appendix 1), with the relative fluorescence intensities $F_2 = 2.4$ and $F_3 = 9.2$. The fluorescence intensity of the free MANT-ATP is taken as $F_1 = 1$. The maximum fluorescence increase of the nucleotide has been determined in the equilibrium fluorescence titration as $\Delta F_{max} = 1.73$ (data not shown). The rate constants are the same as those obtained from the relaxation time analysis (Figure 2, Table 1); A_1 (■), A_2 (□), and A_3 (●).

where F_L^o and F_L^q are the steady-state fluorescence intensities of the of the fluorescent ligand in the absence and presence of the quencher Q, k_q is the bimolecular quenching constant, [Q] is the concentration of the quencher, τ_o is the fluorescence lifetime of the ligand, and $K_{SV}^o = k_q\tau_o$ is the Stern−Volmer quenching constant (*17*−*19*).

Equation 3 describes the effect of the collisional quencher on the fluorescence of the free ligand molecule in solution. An analogous equation can be derived for any intermediate of the reaction in terms of the relative molar fluorescence intensities obtained from the amplitude analyses of the relaxation process. The relative molar fluorescence intensity of an *i*th intermediate, F_i, in the absence of the quencher, is

$$F_i = \frac{I_i}{F_L^o} \tag{4}$$

where I_i is the absolute fluorescence intensity of the intermediate. The amplitude analysis directly provides this ratio (*20*−*23*). In the presence of the quencher, the absolute molar fluorescence intensity of the *i*th intermediate, I_i^q, is defined as

$$I_i^q = \frac{I_i}{1 + K_{SV_i}[Q]} \tag{5}$$

where K_{SV_i} is the Stern−Volmer quenching constant of an *i*th intermediate. Therefore, the relative molar fluorescence intensity of the intermediate, F_q, directly determined from the amplitude analysis of kinetic data obtained in the presence of the quencher, is

$$F_q = \frac{I_i^q}{F_L^q} = \frac{I_i\,(1 + K_{SV}^o[Q])}{F_L^o(1 + K_{SV_i}[Q])} \tag{6}$$

Table 1: Kinetic, Thermodynamic, and Spectroscopic Parameters Characterizing the Binding of MANT-ATP to the DnaC Protein in Buffer T4 (pH 8, 20 °C) Containing Different Acrylamide Concentrations

acrylamide (mM)	k_1 (s^{-1})	k_{-1} (s^{-1})	k_2 (M^{-1} s^{-1})	k_{-2} (s^{-1})	k_3 (s^{-1})	k_{-3} (s^{-1})	K_1	K_2 (M^{-1})	K_3	K_{ov} (M^{-1})	F_2[a]	F_3[a]
0	2.4 ± 0.5	0.6 ± 0.1	(7.2 ± 1.5) × 10^5	1.7 ± 0.2	0.0015 ± 0.0005	0.024 ± 0.005	4 ± 1.8	(4 ± 1.8) × 10^5	0.063 ± 0.02	(3.3 ± 1.5) × 10^5	2.4 ± 0.11	8.64 ± 0.21
10	2.1 ± 0.5	0.65 ± 0.1	(6.6 ± 1.2) × 10^5	1.7 ± 0.2	0.0015 ± 0.0005	0.024 ± 0.003	3.2 ± 1.5	(4 ± 1.8) × 10^5	0.063 ± 0.032	(3.3 ± 1) × 10^5	2.4 ± 0.1	9 ± 0.2
20	2 ± 0.5	0.61 ± 0.1	(6.3 ± 1.1) × 10^5	1.5 ± 0.2	0.0012 ± 0.0003	0.024 ± 0.003	3.3 ± 1.5	(4.2 ± 1.8) × 10^5	0.05 ± 0.032	(3.4 ± 1.5) × 10^5	2.4 ± 0.1	9.2 ± 0.2
35	2 ± 0.5	0.8 ± 0.1	(5.3 ± 1.5) × 10^5	1.3 ± 0.3	0.0013 ± 0.0003	0.028 ± 0.005	2.5 ± 1.5	(4.1 ± 1.8) × 10^5	0.047 ± 0.031	(3.1 ± 1.5) × 10^5	2.38 ± 0.15	9.41 ± 0.2
50	2.1 ± 0.5	0.69 ± 0.1	(5.4 ± 1.5) × 10^5	1.35 ± 0.3	0.0012 ± 0.0003	0.0275 ± 0.005	3.05 ± 1.5	(4 ± 1.8) × 10^5	0.042 ± 0.031	(3.1 ± 1.5) × 10^5	2.39 ± 0.15	9.91 ± 0.2

[a] Values relative to the fluorescence, $F_1 = 1$, of the free MANT-ATP (details in text).

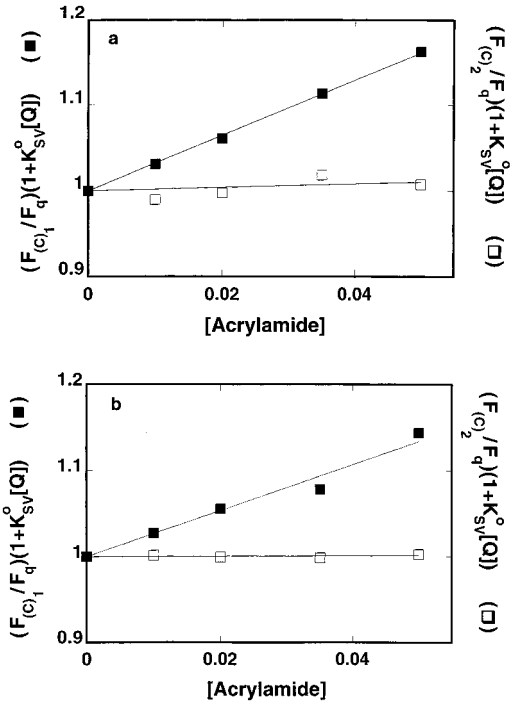

FIGURE 4: (a) Stern−Volmer plots of fluorescence quenching (λ_{ex} = 356 nm, λ_{em} > 400 nm) for the first $(C)_1$ (■) and the second $(C)_2$ (□) intermediate in the intrinsic binding of MANT-ATP to the DnaC protein in buffer T4 (pH 8.1, 20 °C) containing 100 mM NaCl. The relative molar fluorescence intensities of the intermediates at different acrylamide concentrations are from Table 1. The solid lines are linear, least-squares fits of the intermediate Stern−Volmer equation (eq 8 in text) to the data points using $K_{SV_1} = 3.2$ M^{-1} (■) and $K_{SV_2} = 0.21$ M^{-1} (□). (b) Stern−Volmer plots of fluorescence quenching ($\lambda_{ex} = 356$ nm, $\lambda_{em} > 450$ nm) for the first $(C)_1$ (■) and the second $(C)_2$ (□) intermediate in the intrinsic binding of MANT-ADP to the DnaC protein in buffer T4 (pH 8.1, 20 °C) containing 100 mM NaCl. The relative molar fluorescence intensities of the intermediates at different acrylamide concentrations are from Table 2. The solid lines are linear, least-squares fits of the intermediate Stern−Volmer equation (eq 8 in text) to the data points using $K_{SV_1} = 2.7$ M^{-1} (■) and $K_{SV_2} \approx 0$ (□).

and

$$F_q = \frac{F_i(1 + K^o_{SV}[Q])}{(1 + K_{SV_i}[Q])} \quad (7)$$

Rearranging eq 7 provides the required relationship, analogous to the Stern−Volmer eq 3, in terms of the experimentally determined relative molar fluorescence of the intermediate obtained in the absence and presence of the quencher, F_i and F_q, respectively, as

$$\left(\frac{F_i}{F_q}\right)(1 + K^o_{SV}[Q]) = 1 + K_{SV_i}[Q] \quad (8)$$

Expression 8 is a parametric equation where all quantities, with the exception of K_{SV_i}, are known. The plot of the left side of eq 8, as a function of [Q], is a straight line with the intercept equal to 1 and the slope that is equal to the Stern−Volmer quenching constant, K_{SV_i}, specific for a given *i*th intermediate.

Figure 4a shows plots of eq 8 for the two intermediates, $(C)_1$ and $(C)_2$, in the binding of MANT-ATP to the DnaC protein, using the relative molar fluorescence intensities from Table 1. The Stern−Volmer quenching constant, $K_{SV_i} = 3.12 \pm 0.07$ M^{-1}, for free MANT-ATP has been determined in independent quenching experiments, under the same buffer conditions as those of the kinetic measurements (data not shown). In the case of $(C)_1$, the plot is linear in the examined acrylamide concentration range and provides $K_{SV_1} = 3.2 \pm 0.4$ M^{-1}. The slope of the plot for the $(C)_2$ intermediate gives $K_{SV_2} = 0.21 \pm 0.1$. Thus, the obtained data indicate that in the $(C)_1$ intermediate acrylamide has access to the MANT group virtually the same as to the free MANT-ATP in solution. Transition to $(C)_2$ completely shields the MANT moiety of the bound MANT-ATP from the solvent (see Discussion).

Transient, Dynamic Quenching Studies of MANT-ADP Binding to the DnaC Protein. MANT-ADP binds to the DnaC protein with the same mechanism as MANT-ATP (accompanying paper). Analogous, dynamic quenching experiments of the reaction intermediates, as described above for MANT-ATP, have been performed for MANT-ADP binding to the DnaC protein (data not shown). The obtained results are included in Table 2. Similar to MANT-ATP, the relative molar fluorescence intensities F_2 and F_3, characterizing the intermediates $(C)_1$ and $(C)_2$ in MANT-ADP binding, differ significantly in their response to the presence of the dynamic quencher, acrylamide, in solution. The increasing concentration of acrylamide has little effect on the value of $F_2 = 2.16 \pm 0.15$. However, F_3 steadily increases with the increased [acrylamide] from the value of 7.25 ± 0.21, obtained in the absence of acrylamide, to the value of 8.3 ± 0.2, obtained in the presence of 50 mM acrylamide (Table 2). Stern−Volmer plots (eq 8) for the two intermediates, $(C)_1$ and $(C)_2$, in the binding of MANT-ADP to the DnaC protein are shown in Figure 4b. The Stern−Volmer quenching constant, $K^o_{SV} = 2.96 \pm 0.07$ M^{-1}, for free MANT-ADP has been determined in independent quenching experiments (data not shown). The linear plot of the quenching of the $(C)_1$ intermediate fluorescence is characterized by $K_{SV_1} = 2.7 \pm 0.5$ M^{-1}, which is very close to the value of the Stern−Volmer quenching constant obtained for the free nucleotide, as previously observed for MANT-ATP. These data indicate that in the $(C)_1$ intermediate acrylamide has access to the MANT group, similar to the free MANT-ADP in solution. On the other hand, $K_{SV_2} \approx 0$ for the $(C)_2$ intermediate indicates that, in the final intermediate, the MANT moiety of the bound MANT-ADP has no access to the solvent (see Discussion).

Fluorescence Anisotropy, Stopped-Flow Studies of the Nucleotide Cofactor Dynamics in the DnaC Protein Nucleotide-Binding Site. In the stopped-flow kinetic experiments described above and in the accompanying paper, the dynamics of the time-dependent population distribution of different fluorescing ligand species was followed by monitoring the total emission of the sample (Materials & Methods). This has been accomplished by exciting the sample with the vertically polarized light and monitoring the time development of the function

$$F_{Tot}(t) = I_{VV}(t) + 2GI_{VH}(t) \quad (9)$$

were I_{VV} is the fluorescence intensity and the first and second subscripts refer to vertical (V) polarization of the excitation and vertical (V) or horizontal (H) polarization of the emitted

Table 2: Kinetic, Thermodynamic, and Spectroscopic Parameters Characterizing the Binding of MANT-ADP to the DnaC Protein in Buffer T4 (pH 8, 20 °C) Containing Different Acrylamide Concentrations

acrylamide (mM)	k_1 (s^{-1})	k_{-1} (s^{-1})	k_2 (M^{-1} s^{-1})	k_{-2} (s^{-1})	k_3 (s^{-1})	k_{-3} (s^{-1})	K_1	K_2 (M^{-1})	K_3	K_{ov} (M^{-1})	F_2[a]	F_3[a]
0	2.4 ± 0.5	0.6 ± 0.1	$(1.1 \pm 0.3) \times 10^6$	3 ± 0.3	0.002 ± 0.0005	0.027 ± 0.005	4.2 ± 1.8	$(3.7 \pm 1.5) \times 10^5$	0.074 ± 0.04	$(3.3 \pm 1.2) \times 10^5$	2.16 ± 0.15	7.25 ± 0.21
10	2.4 ± 0.5	0.64 ± 0.1	$(9.5 \pm 0.9) \times 10^5$	2.5 ± 0.2	0.0018 ± 0.0004	0.026 ± 0.004	3.75 ± 1.8	$(3.8 \pm 2.1) \times 10^5$	0.069 ± 0.03	$(3.2 \pm 1.2) \times 10^5$	2.14 ± 0.15	7.45 ± 0.2
20	2.4 ± 0.5	0.52 ± 0.1	$(9.2 \pm 0.9) \times 10^5$	2.5 ± 0.2	0.0014 ± 0.0004	0.026 ± 0.004	4.62 ± 1.8)	$(3.68 \pm 2) \times 10^5$	0.054 ± 0.03	$(3.18 \pm 1.5) \times 10^5$	2.14 ± 0.15	7.68 ± 0.2
35	2.4 ± 0.5	0.53 ± 0.1	$(1.33 \pm 1.5) \times 10^5$	3 ± 0.3	0.0012 ± 0.0003	0.026 ± 0.005	4.7 ± 1.8	$(3.8 \pm 2.1) \times 10^5$	0.055 ± 0.03	$(3.7 \pm 1.5) \times 10^5$	2.14 ± 0.15	8 ± 0.2
50	2.4 ± 0.5	0.51 ± 0.1	$(8 \pm 1.5) \times 10^5$	2.3 ± 0.3	0.0011 ± 0.0003	0.026 ± 0.005	4.71 ± 1.8	$(3.48 \pm 1.9) \times 10^5$	0.042 ± 0.025	$(3.9 \pm 1.5) \times 10^5$	2.14 ± 0.15	8.3 ± 0.2

[a] Values relative to the fluorescence, $F_1 = 1$, of the free MANT-ADP (details in text).

light. The factor $G = I_{HV}/I_{HH}$ corrects for the different sensitivity of the emission monochromator for vertically and horizontally polarized light (*18*). Examination of the time-dependence of F_{Tot} allowed us to determine the mechanism of the nucleotide binding (accompanying paper). Amplitude analysis, using the matrix projection operator method, provided relative molar intensities characterizing each individual intermediate of the reaction (accompanying paper, *20*−*23*). For the stopped-flow experiments, performed under pseudo-first-order conditions with respect to the DnaC protein concentration, the total emission is defined in terms of the original coefficient matrix of the reaction, $\mathbf{M_2}$, and the relative molar fluorescence intensities of each individual intermediate, F_1, F_2, and F_3 (*20*−*24*) as

$$F_{Tot}(t) = (F_1 \quad F_2 \quad F_3)e^{\mathbf{M_2}t}\begin{pmatrix} N_{Tot} \\ 0 \\ 0 \end{pmatrix} \qquad (10)$$

Expanding the matrix $e^{\mathbf{M_2}t}$ using its projection operators provides the total emission as a function of the molar fluorescence intensities of each individual intermediate and the eigenvalues of the coefficient matrix, $\mathbf{M_2}$, as (accompanying paper)

$$F_{Tot}(t) = (F_1 \quad F_2 \quad F_3)\begin{pmatrix} S_{01} & S_{11} & S_{21} \\ S_{02} & S_{12} & S_{22} \\ S_{03} & S_{13} & S_{23} \end{pmatrix}\begin{bmatrix} 1 \\ \exp(\lambda_1 t) \\ \exp(\lambda_2 t) \end{bmatrix} \qquad (11)$$

The relaxation times of the observed kinetic process are then $\tau_1 = -1/\lambda_1$ and $\tau_2 = -1/\lambda_2$, respectively (*20*−*24*). Molar fluorescence intensities provide information about the physical environment surrounding the fluorophore (accompanying paper) (*25*, *26*). Information about the mobility of the fluorescing ligand, during the fluorescence lifetime of the individual intermediates, can be obtained by examining the time dependence of the fluorescence anisotropy in the stopped-flow experiments (*18*, *27*). The fluorescence lifetime of the MANT group is ~3.9 ns (*14*). Because the lifetime of the fluorescing ligand is orders of magnitude shorter than the lifetime of any intermediate formed in the kinetic reaction, the fluorescence anisotropy stopped-flow studies provide the steady-state anisotropy of the ligand molecule in each intermediate.

Contrary to the total emission, the time-dependent fluorescence anisotropy in a chemical reaction is not a simple sum of exponential functions (*18*, *27*). An excellent discussion of the application of the fluorescence anisotropy to examine the reaction mechanism has been previously described (*27*). However, our approach is different. We know the mechanism of MANT-ATP and MANT-ADP binding to the DnaC protein from the total emission studies (accompanying paper). Our task is to extract the steady-state anisotropies of the ligand molecule (MANT-ATP and MANT-ADP) in each intermediate of the reaction with the macromolecule (DnaC) from the fluorescence anisotropy stopped-flow data. This can be conveniently accomplished by using the matrix projection operator formalism (*20*−*23*).

The time course of the fluorescence anisotropy of a fluorescing sample examined in stopped-flow experiments is a more complex function than the total emission and, in general, is defined as

$$r(t) = \frac{I_{VV}(t) - I_{VH}(t)}{I_{VV}(t) + 2GI_{VH}(t)} \quad (12)$$

where the denominator is the total emission defined by eq 9. Algebraic manipulations of eq 12 provide

$$r(t) = \sum_{i=1}^{n} f_i(t) r_i \quad (13)$$

where $f_i(t)$ is the time-dependent fractional contribution of ith fluorescing species to the total emission of the sample and r_i is its corresponding steady-state fluorescence anisotropy.

For the specific mechanism of MANT-nucleotide binding to the DnaC protein, defined by eq 2, relationship 13 takes form as

$$r(t) = f_N(t) r_N + f_{C_1}(t) r_{C_1} + f_{C_2}(t) r_{C_2} \quad (14)$$

where r_N, r_{C_1}, and r_{C_2} are steady-state anisotropies of the free MANT-nucleotide and $(C)_1$ and $(C)_2$ intermediates. Using the original coefficient matrix of the reaction, $\mathbf{M_2}$, the time course of the anisotropy in eq 14 is defined as

$$r(t) = \frac{(r_N F_1 \quad r_{C_1} F_2 \quad r_{C_2} F_3)\, e^{\mathbf{M_2 t}} \begin{pmatrix} N_{Tot} \\ 0 \\ 0 \end{pmatrix}}{(F_1 \quad F_2 \quad F_3) e^{\mathbf{M_2 t}} \begin{pmatrix} N_{Tot} \\ 0 \\ 0 \end{pmatrix}} \quad (15)$$

Expanding the $e^{\mathbf{M_2 t}}$ matrix and using its projection operators provides (accompanying paper, *20*−*23*)

$$r(t) = \frac{(r_N F_1 \quad r_{C_1} F_2 \quad r_{C_2} F_3) \begin{pmatrix} S_{01} & S_{11} & S_{21} \\ S_{02} & S_{12} & S_{22} \\ S_{03} & S_{13} & S_{23} \end{pmatrix} \begin{pmatrix} 1 \\ \exp(\lambda_1 t) \\ \exp(\lambda_2 t) \end{pmatrix}}{(F_1 \quad F_2 \quad F_3) \begin{pmatrix} S_{01} & S_{11} & S_{21} \\ S_{02} & S_{12} & S_{22} \\ S_{03} & S_{13} & S_{23} \end{pmatrix} \begin{pmatrix} 1 \\ \exp(\lambda_1 t) \\ \exp(\lambda_2 t) \end{pmatrix}} \quad (16)$$

Equation 16 describes the experimentally observed time dependence of the fluorescence anisotropy in the binding of MANT-ATP or MANT-ADP to the DnaC protein under pseudo-first-order conditions with respect to the protein concentration. The anisotropy is expressed using the relative molar fluorescence intensities and anisotropies of individual intermediates of the reaction and the eigenvalues (reciprocal relaxation times) of the coefficient matrix. Notice that, in general, once the coefficient matrix **M** for a given reaction mechanism is obtained, the projection operators are defined using Sylvester's theorem (*20*−*23*, *28*). The total emission and anisotropy can then be defined without the determination of the eigenvectors of **M**. For complex mechanisms, the numerical analysis is limited to the determination of only the eigenvalues of **M** (*20*−*23*). The generalization of this expression to any kinetic mechanism is straightforward.

The stopped-flow traces of MANT-ADP fluorescence anisotropy, after mixing 5×10^{-7} M nucleotide with different DnaC protein concentrations in buffer T4 (pH 8.1, 20 °C) containing 100 mM NaCl, are shown in Figure 5. The kinetic trace has been collected in two time bases, 1 and 200 s. The anisotropy rises from the value corresponding to the free MANT-ADP at time $t \approx 0$ of the reaction to the value corresponding to the anisotropy of the completely bound nucleotide ($r = 0.183 \pm 0.005$), weighted by the degree of cofactor saturation at an applied protein concentration. The anisotropy kinetic trace seems to be the sum of the exponential functions; however, as we discussed above, it is, in fact, described by a more complex expression, defined by eq 16.

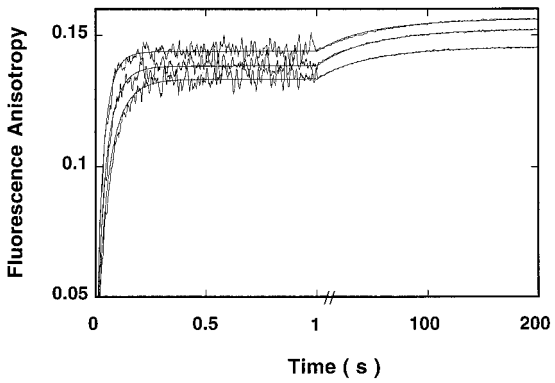

FIGURE 5: Fluorescence anisotropy stopped-flow kinetic traces (λ_{ex} = 356 nm, λ_{em} > 400 nm) recorded in two time bases, 1 and 200 s, after mixing MANT-ADP with the DnaC protein in buffer T4 (pH 8.1, 20 °C) containing 100 NaCl. The final concentration of the nucleotide is 5×10^{-7} M. The final concentrations of the protein, from bottom to top, are 1.1×10^{-5}, 1.47×10^{-5}, and 2.02×10^{-5} M. The solid lines are the nonlinear, least-squares fits of the experimental curve to eq 16 using $r_{C_1} = 0.1491$ and $r_{C_2} = 0.1775$, $r_{C_1} = 0.1506$ and $r_{C_2} = 0.1872$, and $r_{C_1} = 0.1533$ and $r_{C_2} = 0.1856$. The value of steady-state anisotropy of the free MANT-ADP is $r_N = 0.015$ (14). The rate constants and relative molar fluorescence intensities are the same as included in Table 4 for the same solution conditions.

The analysis of the experimental kinetic traces in Figure 5 is significantly facilitated by the fact that F_1, F_2, F_3, and the rate constants that define the eigenvalues of the coefficient matrix are known from the total emission studies (see above and accompanying paper). From our previous studies, we know that the free MANT-ATP anisotropy is $r_N = 0.015 \pm 0.005$ (*14*). Thus, there are two parameters that must be determined, r_{C_1} and r_{C_2}. The solid lines in Figure 5 are nonlinear, least-squares fits of the experimental fluorescence anisotropy curves, using eq 16, with anisotropies of the intermediates C_1 and C_2 as fitting parameters. The values of r_{C_1} and r_{C_2}, obtained at different protein concentrations, are very close (Figure 5). This is an expected result because at any protein concentration the same intermediates, characterized by the same fluorescence anisotropy, are observed. The obtained values of r_{C_1} and r_{C_2} for MANT-ADP-DnaC intermediates averaged over all protein concentrations applied are $r_{C_1} = 0.151 \pm 0.005$ and $r_{C_2} = 0.183 \pm 0.005$.

Analogous stopped-flow fluorescence anisotropy experiments have been performed for the MANT-ATP-DnaC system (data not shown). To extract steady-state anisotropies of the reaction intermediates, we have analyzed the experimental kinetic curves in the same way as described above for MANT-ADP. Here we also utilize the fact that F_1, F_2, F_3, and the rate constants for MANT-ATP binding to the DnaC protein are known from the total emission studies (see

above and accompanying paper). The determined values for MANT-ATP are $r_{C_1} = 0.150 \pm 0.005$ and $r_{C_2} = 0.190 \pm 0.005$.

The obtained results strongly indicate that the formation of the $(C)_1$ intermediate is already accompanied by a significant immobilization of both MANT-ADP and MANT-ATP in the nucleotide-binding site of the DnaC protein. The values of the fluorescence anisotropy of the intermediate indicate that the mobility of both ATP and ADP analogues is similarly restricted. Further increase of the anisotropy in the formation of $(C)_2$ suggests a further restriction of both MANT-ATP and MANT-ADP mobility (see Discussion).

Salt Effect on the Dynamics of the MANT-ATP and MANT-ADP Binding to the DnaC Protein. Recent equilibrium studies indicate that the binding of MANT-ATP and MANT-ADP to the DnaC protein is affected by the salt concentration in solution (*11*). As the salt concentration increases, the affinity of the nucleotide cofactors decreases. The dependence of the logarithm of the overall equilibrium constants, $K_{MANT-ATP}$ and $K_{MANT-ADP}$, upon the logarithm of [NaCl] (log−log plot, (*29*)) is characterized by the slopes $\partial \log K_{MANT-ATP}/\partial \log[NaCl] = -0.7 \pm 0.1$ and $\partial \log K_{MANT-ADP}/\partial \log[NaCl] = -1 \pm 0.1$ and indicates that the net release of ~1 ion accompanies the formation of both complexes (*29*).

Further insight into the nature of the observed conformational transitions and formed intermediates can be obtained by examining the salt effect on the kinetics of the binding of the nucleotide cofactors to the DnaC protein. The stopped-flow kinetic experiments were performed in the same salt concentration range as the equilibrium titration studies (*11*). To access all relaxation processes characterizing DnaC preequilibrium transition and intrinsic nucleotide-binding steps, we conducted the experiments under pseudo-first-order conditions with respect to the nucleotide concentration (accompanying paper). The kinetic data were analogously analyzed, as described in the accompanying paper. The obtained rate constants, partial equilibrium constants, and spectroscopic parameters are included in Tables 3 and 4 for MANT-ATP and MANT-ADP, respectively.

The data in Tables 3 and 4 indicate that the rate constants k_1 and k_{-1}, characterizing the conformational transition of the DnaC protein prior to the nucleotide binding, are affected very little by the salt in solution. Similar behavior of rate constants k_1 and k_{-1}, observed for both MANT-ATP and MANT-ADP, results from the fact that the same protein conformational transition is observed. However, for both cofactors, the changing salt concentration significantly affects the dynamics of the formation of the $(C)_1$ intermediate. In the case of MANT-ADP, the rate constant k_2 decreases from $(1.8 \pm 0.3) \times 10^6$ M^{-1} s^{-1} in 25 mM NaCl to $(7.2 \pm 1.5) \times 10^5$ M^{-1} s^{-1} in the presence of 200 mM NaCl. Also, the rate constant k_{-2}, characterizing the release of the nucleotide from the $(C)_1$ intermediate back to the solution, increases for both cofactors with the increasing salt concentration. On the other hand, the dynamics of the slowest step, characterized by k_3 and k_{-3}, is only slightly affected by the salt with both rate constants increasing with the increased [NaCl].

The dependence of the logarithm of the partial equilibrium constant K_1, characterizing the conformational transition of the DnaC protein prior to MANT-ADP binding, upon the logarithm of [NaCl] (log−log plot) is shown in Figure 6a. The slope of the plot $\partial \log K_1/\partial \log[NaCl] = -0.02 \pm 0.2$

Table 3: Kinetic, Thermodynamic, and Spectroscopic Parameters Characterizing the Binding of MANT-ATP to the DnaC Protein in Buffer T4 (pH 8, 20 °C) Containing Different NaCl Concentrations

NaCl (mM)	k_1 (s^{-1})	k_{-1} (s^{-1})	k_2 (M^{-1} s^{-1})	k_{-2} (s^{-1})	k_3 (s^{-1})	k_{-3} (s^{-1})	K_1	K_2 (M^{-1})	K_3	K_{ov} (M^{-1})	F_2[a]	F_3[a]
25	1.7 ± 0.5	0.4 ± 0.1	(1.4 ± 1.5) × 10^6	1.2 ± 0.3	0.0012 ± 0.0003	0.019 ± 0.005	4.25 ± 1.8	(1.15 ± 1.8) × 10^5	0.063 ± 0.023	(9.9 ± 4) × 10^5	2.48 ± 0.12	9.3 ± 0.15
50	1.8 ± 0.4	0.45 ± 0.1	(1.1 ± 2) × 10^6	1.8 ± 0.3	0.0013 ± 0.0003	0.02 ± 0.005	4 ± 1.9	(6.1 ± 1.8) × 10^5	0.065 ± 0.02	(5.2 ± 1.8) × 10^5	2.47 ± 0.15	8.93 ± 0.2
100	2.4 ± 0.5	0.6 ± 0.1	(7.2 ± 1.5) × 10^5	1.7 ± 0.2	0.0015 ± 0.0005	0.024 ± 0.005	4 ± 1.8	(4 ± 1.8) × 10^5	0.063 ± 0.02	(3.3 ± 1.5) × 10^5	2.4 ± 0.11	8.64 ± 0.21
200	2.2 ± 0.5	0.55 ± 0.1	(4 ± 1.2) × 10^5	2.1 ± 0.3	0.002 ± 0.0005	0.026 ± 0.005	4 ± 1.9	(1.9 ± 0.6) × 10^5	0.077 ± 0.04	(1.64 ± 1.53) × 10^5	2.43 ± 0.15	7.35 ± 0.21

[a] Values relative to the fluorescence, $F_1 = 1$, of the free MANT-ADP (details in text).

Table 4: Kinetic, Thermodynamic, and Spectroscopic Parameters Characterizing the Binding of MANT-ADP to the DnaC Protein in Buffer T4 (pH 8, 20 °C) Containing Different NaCl Concentrations

NaCl (mM)	k_1 (s^{-1})	k_{-1} (s^{-1})	k_2 (M^{-1} s^{-1})	k_{-2} (s^{-1})	k_3 (s^{-1})	k_{-3} (s^{-1})	K_1	K_2 (M^{-1})	K_3	K_{ov} (M^{-1})	F_2[a]	F_3[a]
25	1.7 ± 0.4	0.4 ± 0.1	(1.8 ± 0.3) × 10^6	1.6 ± 0.3	0.0014 ± 0.0003	0.021 ± 0.005	4.3 ± 1.5)	(1.13 ± 1.5) × 10^5	0.067 ± 0.023	(9.7 ± 1) × 10^5	2.33 ± 0.1	7.67 ± 0.23
50	2.3 ± 0.5	0.55 ± 0.1	(1.6 ± 0.3) × 10^6	2.8 ± 0.3	0.0016 ± 0.0003	0.023 ± 0.005	4.2 ± 1.9	(5.7 ± 1.8) × 10^5	0.071 ± 0.04	(4.9 ± 1.6) × 10^5	2.24 ± 0.15	7.78 ± 0.21
100	2.4 ± 0.5	0.6 ± 0.1	(1.1 ± 0.3) × 10^6	3 ± 0.3	0.002 ± 0.0005	0.027 ± 0.005	4.2 ± 1.8	(3.7 ± 1.5) × 10^5	0.074 ± 0.04	(3.3 ± 1.2) × 10^5	2.16 ± 0.15	7.25 ± 0.21
150	2.4 ± 0.5	0.4 ± 0.1	(8.8 ± 1.5) × 10^5	4 ± 0.3	0.0015 ± 0.0003	0.026 ± 0.005	6 ± 2.5	(2.2 ± 1) × 10^5	0.058 ± 0.03	(2 ± 0.8) × 10^5	2.26 ± 0.15	7.71 ± 0.21
200	1.8 ± 0.5	0.5 ± 0.1	(7.2 ± 1.5) × 10^5	4 ± 0.3	0.0017 ± 0.003	0.027 ± 0.005	3.6 ± 1.5	(1.8 ± 0.9) × 10^5	0.063 ± 0.03	(1.5 ± 0.7) × 10^5	2.18 ± 0.15	7.42 ± 0.23

[a] Values relative to the fluorescence, $F_1 = 1$, of the free MANT-ADP (details in text).

indicates that no net release of ions accompanies the transition $(DnaC)_1 \leftrightarrow (DnaC)_2$. The dependence of the logarithm of the partial equilibrium constant K_3, which characterizes the $(C)_1 \leftrightarrow (C)_2$ step, upon the logarithm of [NaCl] (log−log plot) is also included in Figure 6a. The slope of the plot is $\partial \log K_3/\partial \log[NaCl] = 0.08 \pm 0.2$. Thus, no net release of ions accompanies the formation of $(C)_1 \leftrightarrow (C)_2$. However, contrary to K_1 and K_3, the value of K_2, characterizing the formation of the first intermediate in MANT-ADP binding to the DnaC protein, $(C)_1$, shows a significant dependence on salt. The log−log plot for equilibrium constant K_2 is shown in Figure 6b. The plot is characterized by the slope $\partial \log K_2/\partial \log[NaCl] = -0.84 \pm 0.25$, indicating a net release of ∼1 ions in the formation of the $(C)_1$ intermediate. The analogous analysis of the salt effect on the partial equilibrium constants characterizing the DnaC protein conformational transition and the intrinsic nucleotide binding has been performed for MANT-ATP-DnaC interactions. The corresponding log−log plots are shown in Figure 6c,d. The obtained slopes of the plots are $\partial \log K_1/\partial \log[NaCl] = 0.02 \pm 0.2$, $0.\partial \log K_2/\partial \log[NaCl] = -0.87 \pm 0.25$, and $\partial \log K_3/\partial \log[NaCl] = -0.05 \pm 0.2$. Thus, it is evident that the ion release accompanying MANT-ADP and MANT-ATP binding to the DnaC protein predominantly occurs in the formation of the first nucleotide intermediate $(C)_1$.

The almost identical values of the net ion release, obtained from the salt dependence of the overall binding constants, $K_{MANT-ATP}$ or $K_{MANT-ADP}$, and the corresponding partial equilibrium constants, K_1, K_2, and K_3, suggest that the overall net ion release is a simple sum of the ion release in partial reactions. However, it should be pointed out that this is generally not the case (*23*, *29*). For the considered mechanism of MANT-ATP and MANT-ADP binding to the DnaC protein, defined by eq 2, the value of the overall equilibrium, K_N, is related to the partial equilibrium constants by (accompanying paper)

$$K_N = \frac{K_1 K_2 (1 + K_3)}{1 + K_1} \tag{17}$$

The derivative of the logarithm of K_N, with respect to the logarithm of [NaCl], is then

$$n = \frac{\partial \log K_N}{\partial \log[NaCl]} = \left[\frac{1}{1 + K_1}\right] n_1 + n_2 + \left[\frac{K_3}{1 + K_3}\right] n_3 \tag{18}$$

where $n_1 = \partial \log K_1/\partial \log[NaCl]$, $n_2 = \partial \log K_2/\partial \log[NaCl]$, and $n_3 = \partial \log K_3/\partial \log[NaCl]$ are the numbers of ions released in the partial reaction for the formation of $(DnaC)_1$, $(C)_1$, and $(C)_2$ intermediates. Because for the DnaC−nucleotide system n_1 and n_3 both equal ∼0, the value of n is $\sim n_2$, i.e., the net ion release in the formation of the first intermediate in the intrinsic nucleotide binding to the DnaC protein.

Comparison of the relative molar fluorescence intensities for MANT-ATP and MANT-ADP binding to the DnaC protein, obtained at different salt concentrations, indicates that for both cofactors the value of F_2 that characterizes the $(C)_1$ intermediate is not affected by the increasing salt concentration in solution (Tables 3 and 4). However, there is clear difference between the ATP and ADP cofactor in the salt effect on the F_3. While in the case of MANT-ADP the relative molar fluorescence intensity of the $(C)_2$ inter-

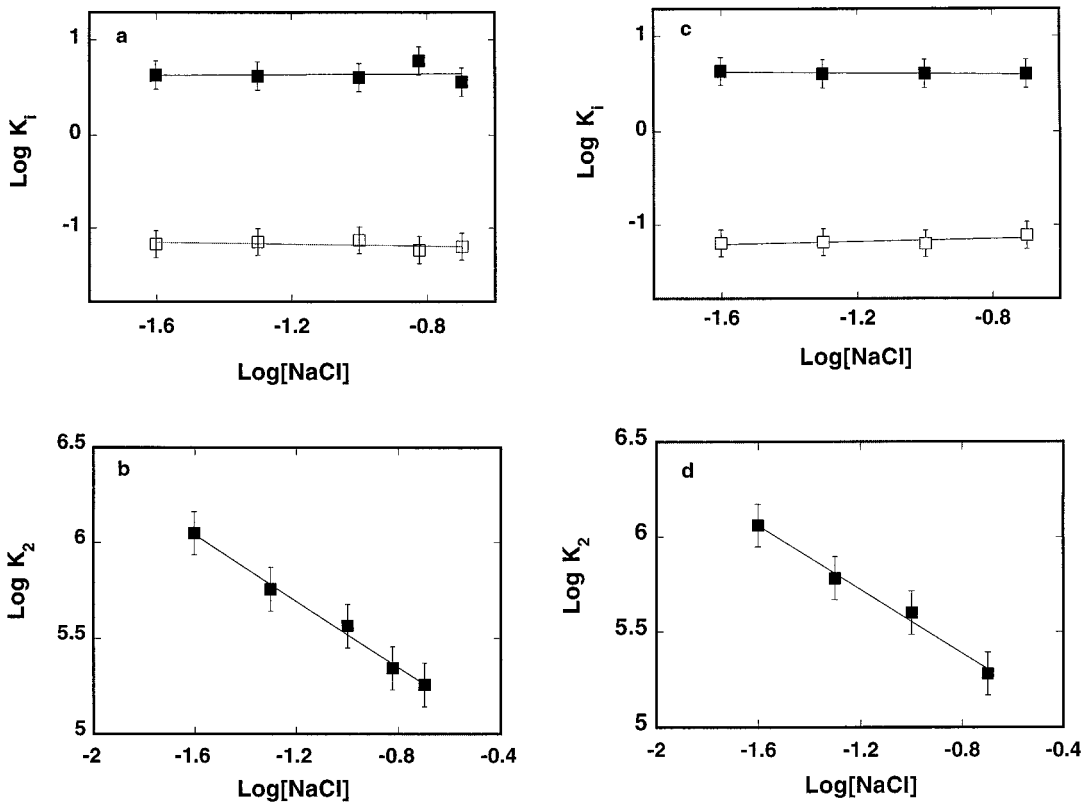

FIGURE 6: (a) Dependence of the partial equilibrium constants K_1 (■) and K_3 (□), characterizing the conformational transition of the DnaC protein prior to the nucleotide binding and the second step in the intrinsic MANT-ADP binding (eq 2), upon the log[NaCl] (log−log plots). The plots are characterized by the slopes $\partial\log K_1/\partial\log[\mathrm{NaCl}] = -0.02 \pm 0.2$ and $\partial\log K_3/\partial\log[\mathrm{NaCl}] = 0.08 \pm 0.2$, respectively. (b) The dependence of the partial equilibrium constant K_2 (■), characterizing the bimolecular step in the intrinsic MANT-ADP binding (eq 2), upon the log[NaCl] (log−log plots). The plot is described by the slope $\partial\log K_2/\partial\log[\mathrm{NaCl}] = -0.84 \pm 0.25$. (c) The dependence of the partial equilibrium constants K_1 (■) and K_3 (□), characterizing the conformational transition of the DnaC protein prior to the nucleotide binding and the second step in the intrinsic MANT-ATP binding (eq 2), upon the log[NaCl] (log−log plots). The plots are characterized by the slopes $\partial\log K_1/\partial\log[\mathrm{NaCl}] = 0.02 \pm 0.2$ and $\partial\log K_3/\partial\log[\mathrm{NaCl}] = -0.05 \pm 0.2$, respectively. (d) The dependence of the partial equilibrium constant K_2 (■), characterizing the bimolecular step in the intrinsic MANT-ATP binding (eq 2), upon the log[NaCl] (log−log plots). The plot is described by the slope $\partial\log K_2/\partial\log[\mathrm{NaCl}] = -0.87 \pm 0.25$.

mediate is not affected by salt, the same parameter significantly decreases with the increasing [NaCl] for MANT-ATP (Tables 3 and 4). Thus, although the salt effect on the energetics of the overall binding process and the partial steps in MANT-ATP and MANT-ADP association with the DnaC protein are very similar, the structural environments of MANT-ATP and MANT-ADP are affected differently in the $(C)_2$ intermediates for both cofactors (see Discussion).

Temperature Effect on MANT-ATP and MANT-ADP Binding to the DnaC Protein. Fluorescence titration of MANT-ATP with the DnaC protein at two different temperatures, 10 and 25 °C, in buffer T4 (pH 8.1) containing 100 mM NaCl, are shown in Figure 7. The solid lines are computer fits of the isotherms to the single binding-site isotherm, $\Delta F = \Delta F_{max}\{K_{MANT-ATP}\ [DnaC]/(1 + K_{MANT-ATP}\ [DnaC]\}$ (Figure 7) (*11*). It is evident that temperature has a very moderate effect on the overall binding process. The overall binding constant decreases from $(3.5 \pm 0.4) \times 10^5\ M^{-1}$ to $(2.7 \pm 0.4) \times 10^5\ M^{-1}$. The maximum observed fluorescence increase at saturation of the nucleotide with the protein increases from 1.44 ± 0.12 at 10 °C to 1.72 ± 0.15 at 25 °C. The dependence of the overall binding constant, $K_{MANT-ATP}$, upon the temperature is shown in Figure 8a. Using the van't Hoff equation $\partial\ln K/\partial(1/T) = -\Delta H/R$, where ΔH is the enthalpy of the reaction and R is the gas constant, the slope of the plot provides $\Delta H_{ov} = -2.9 \pm 1$ kcal/mol.

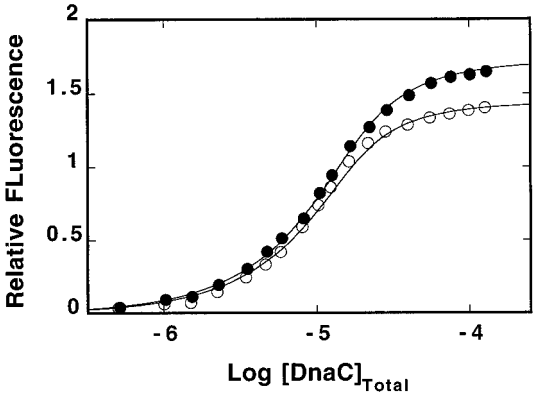

FIGURE 7: Fluorescence titration of MANT-ATP with the DnaC protein in buffer T4 (pH 8.1), containing 100 mM NaCl, at two different temperatures, 10 °C (○) and 25 °C (●). The solid lines are computer fits of the isotherms to the single binding-site isotherm (*11*), $\Delta F = \Delta F_{max}\{K_{MANT-ATP}[DnaC]/(1 + K_{MANT-ATP}[DnaC]\}$ with $\Delta F_{max} = 1.44$, $K_{MANT-ATP} = 3.5 \times 10^5\ M^{-1}$ (10 °C) and with $\Delta F_{max} = 1.72$, $K_{MANT-ATP} = 2.7 \times 10^5\ M^{-1}$ (25 °C), respectively.

The temperature effect on the partial steps in MANT-ATP binding to the DnaC protein has been examined in stopped-flow experiments. The kinetic data have been obtained at the same temperatures as the equilibrium studies. The dependence of the partial equilibrium constant, K_2, characterizing the bimolecular step upon the temperature is included in Figure 8a. The slope of the plot provides $\Delta H_2 = 3.1 \pm$

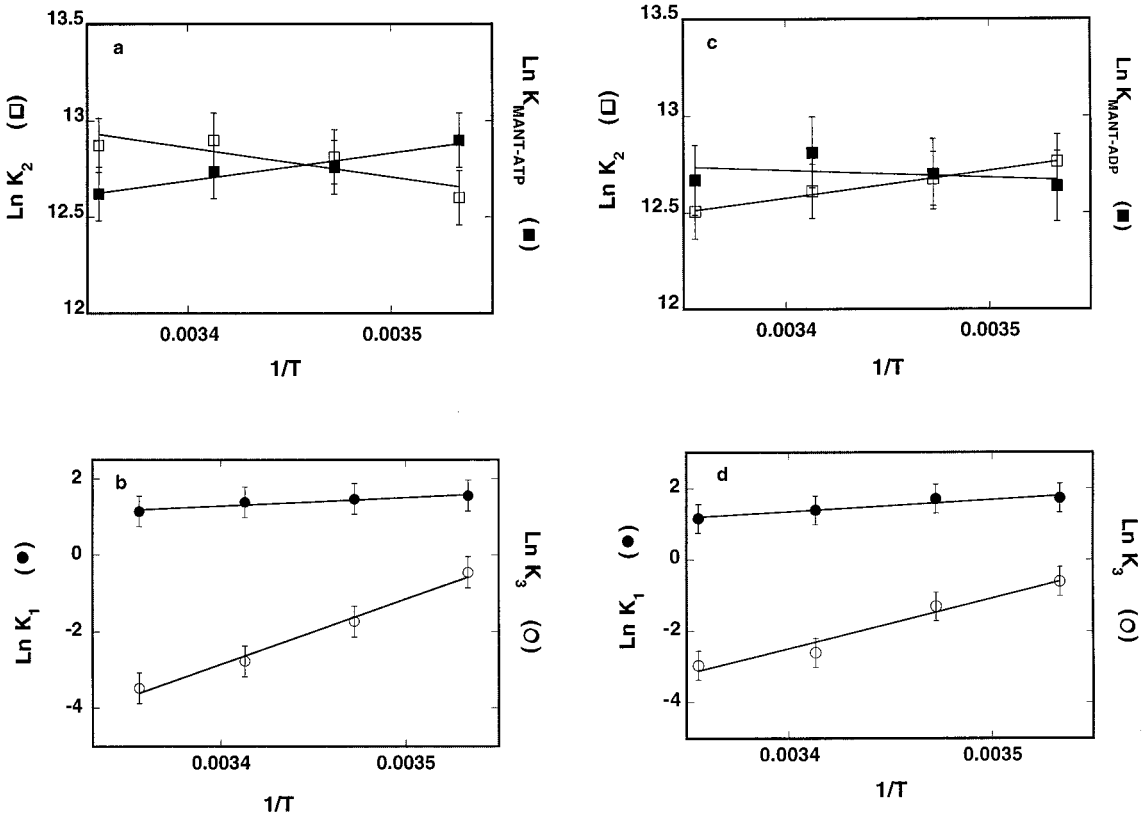

FIGURE 8: (a) Dependence of the natural logarithm of $K_{MANT-ATP}$ (■) and the natural logarithm of the partial equilibrium constant, K_2 (□), characterizing the bimolecular step upon the reciprocal temperature (K). (b) The dependence of the natural logarithm of the partial equilibrium constant K_1 (●), characterizing the preequilibrium conformational transition of the DnaC protein, and the natural logarithm of the partial equilibrium constant K_3 (○), characterizing the $(C)_1 \leftrightarrow (C)_2$ transition upon the reciprocal temperature (K). (c) The dependence of the natural logarithm of $K_{MANT-ADP}$ (■) and the natural logarithm of the partial equilibrium constant K_2 (□), characterizing the bimolecular step, upon the reciprocal temperature (K). (d) The dependence of the natural logarithm of the partial equilibrium constant K_1 (●), characterizing the pre-equilibrium conformational transition of the DnaC protein, and the natural logarithm of the partial equilibrium constant K_3 (○), characterizing the $(C)_1 \leftrightarrow (C)_2$ transition in the binding of MANT-ADP to the DnaC protein, upon the reciprocal temperature (K).

Table 5: Thermodynamic Parameters Characterizing the Overall Binding and Individual Steps in the Binding of MANT-ATP and MANT-ADP Cofactors to the DnaC Protein, According to the Mechanism Defined by Eq 2 (see text) in Buffer T4 (pH 8.1) Containing 100 MM NaCl[a]

cofactor	ΔH^b_{ov} (kcal/mol)	ΔS^b_{ov} (cal/deg)	ΔH_1 (kcal/mol)	ΔS_1 (cal/deg)	ΔH_2 (kcal/mol)	ΔS_2 (cal/mol)	ΔH_3 (kcal/mol)	ΔS_3 (cal/deg)
MANT-ATP	-2.9 ± 1	15.2 ± 4.5	-4.5 ± 2	-12.5 ± 6	3.1 ± 1.5	36 ± 12	-34 ± 15	-121 ± 60
MANT-ADP	-2.8 ± 1	15.2 ± 4.5	-6.8 ± 3	-26 ± 12	0.7 ± 1	28 ± 14	-28 ± 14	-90 ± 45

[a] The errors are standard deviation determined using 3−4 independent experiments. [b] Determined in independent equilibrium titrations.

1.5 kcal/mol. Thus, the bimolecular step behaves very differently from the overall binding process and is characterized by a positive enthalpy change. The dependence of the natural logarithm of the partial equilibrium constant, K_1, characterizing the preequilibrium conformational transition of the DnaC protein and the partial equilibrium constant, K_3, characterizing the $(C)_1 \leftrightarrow (C)_2$ transition upon the temperature is shown in Figure 8b. The slopes of the plots provide $\Delta H_1 = -4.5 \pm 2$ kcal/mol and $\Delta H_3 = -34 \pm 15$ kcal/mol. Although the errors are inherently large for these parameters, the obtained results indicate that both steps are described by a negative enthalpy change, with the value of ΔH_3 being significantly larger. Analogous experiments have been performed for MANT-ADP. The corresponding plots are shown in Figure 8c,d. The obtained apparent thermodynamic parameters characterizing the overall binding step and the partial steps in the binding of both analogues to the DnaC protein are included in Table 5.

The overall enthalpy and entropy changes, ΔH_{ov} and ΔS_{ov}, have favorable contributions to the ΔG°_{ov} for MANT-ATP and MANT-ADP binding to the DnaC protein. However, the data indicate that the values of both parameters result from a complex effect of the thermodynamic characteristics of the partial steps. The pre-equilibrium conformational transition of the DnaC protein is accompanied by apparent negative enthalpy and entropy changes in the examined solution conditions (Table 5). Thus, the process is apparently driven by enthalpy. The bimolecular binding step is accompanied by an unfavorable, positive enthalpy change, particularly for MANT-ATP. On the other hand, for both cofactors, the step is characterized by a large and positive entropy contribution, indicating that the apparent entropy change drives the bimolecular step. The transition $(C)_1 \leftrightarrow (C)_2$ is very different. It is characterized by an apparent large favorable enthalpy change and a very unfavorable large entropy change (see Discussion).

As in the case of the salt effect discussed above, the overall enthalpy and entropy changes are not simple sums of the apparent enthalpy and entropy changes accompanying the partial steps in MANT-ATP and MANT-ADP binding to the DnaC protein. This is evident by comparison of the overall enthalpy and entropy with the corresponding partial parameters (Table 5). Using eq 17, which defined the overall binding constant, K_N, for the cofactor binding to the DnaC protein, we can derive the van't Hoff equation for the overall enthalpy change in the reaction, described by eq 2 as

$$\frac{\partial \ln K_N}{\partial\left(\frac{1}{T}\right)} = -\left(\frac{1}{1+K_1}\right)\frac{\Delta H_1}{R} - \frac{\Delta H_2}{R} - \left(\frac{K_3}{1+K_3}\right)\frac{\Delta H_3}{R} \quad (19)$$

and

$$\Delta H_{ov} = \left(\frac{1}{1+K_1}\right)\Delta H_1 + \Delta H_2 + \left(\frac{K_3}{1+K_3}\right)\Delta H_3 \quad (20)$$

These expressions are analogous to eq 18, with $\Delta H_1 = -R[\partial \ln K_1/\partial(1/T)]$, $\Delta H_2 = -R[\partial \ln K_2/\partial(1/T)]$, and $\Delta H_3 = -R[\partial \ln K_3/\partial(1/T)]$. Introducing the values of the ΔH_1, ΔH_2, and ΔH_3 from Table 5 for MANT-ADP and taking the values of the partial equilibrium constants, K_1, K_2, and K_3, at 20 °C as a reference, we obtain $\Delta H_{ov} \approx -2.6$ kcal/mol. Analogous calculations for MANT-ATP provide $\Delta H_{ov} \approx -0.3$ kcal/mol. These values are lower than the same parameters obtained from independent equilibrium titrations, reflecting the fact that errors on the determination of partial equilibrium constants, and the corresponding enthalpy changes, can be as high as ~50% (Table 5). Nevertheless, they clearly indicate that the overall binding process, composed of three steps with very different enthalpy changes, is only moderately affected by the temperature and is characterized by a low negative enthalpy change, as experimentally determined.

DISCUSSION

Transient Dynamic Quenching of Reaction Intermediates. Fluorescence dynamic quenching is one of the methods most often used to experimentally determine the solvent accessibility of a fluorophore (*17, 18*). The approach is based on adding a quencher to the solution that, as a result of a simple collision, efficiently depletes the excited state of the fluorescing molecule. This is a unique property of fluorescence and results from the fact that an extra radiationless process can be introduced without affecting, to any significant degree, the thermodynamic equilibrium and kinetic properties of the interacting system (*17*−*19*). Previously, we described the theoretical and experimental bases of the method to study equilibrium binding of a ligand to a macromolecule on the basis of induced differential collisional quenching of the intrinsic fluorescence of a ligand or a macromolecule by the presence of an efficient, preferably nonionic, collisional quencher (*19*). In this work we extended the method to examine the dynamics of the interacting system, particularly the solvent accessibility, i.e., the structure of the individual transient intermediates of the reaction.

A prerequisite for the quantitative determination of the quenching efficiency is the amplitude analysis of the relaxation process that provides relative molar fluorescence intensities of all intermediates of the reaction (accompanying paper, *20*−*23*). The relative molar fluorescence intensities are the ratios of the fluorescence intensity of the intermediates to the fluorescence intensity of the free ligand (eq 4). This provides a direct method to quantitatively address the fluorescence quenching of a transient intermediate. In the presence of the quencher, the fluorescence of the free ligand is described by the Stern−Volmer equation that can be determined in independent, fluorescence quenching titrations. The relative molar fluorescence intensity of an intermediate is a function of the quencher concentration, described by eq 8, with a single unknown parameter, the Stern−Volmer quenching constant, K_{SV_i}, specific for the intermediate.

In the First Intermediate in the Nucleotide Association with the DnaC Protein, the Binding Site is Exposed to the Solvent. The first step in the intrinsic binding of nucleotide cofactors to the DnaC protein provides the major part of the free energy of binding (accompanying paper, see above). Recall, the binding site is highly specific for the adenine nucleotides (*11*). The cofactors containing another type of the base have an undetectable affinity. Moreover, the 2′OH group of the ribose is involved in direct interactions in the binding site, as indicated by a 2−3 orders of magnitude lower affinity of dATP and dADP as compared to that for ATP and ADP. Thus, these results indicate that formation of the $(C)_1$ intermediate must include interactions of the adenosine and ribose with the binding site (accompanying paper). However, the Stern−Volmer quenching constant for $(C)_1$ is very close to the value obtained for the free MANT-ATP and MANT-ADP, indicating that the solvent has free access to the MANT group located on the ribose of the bound nucleotide, although the ribose is involved in interactions with the protein. The simplest explanation of these results is that the nucleotide-binding site of the DnaC protein is located on the surface of the protein, completely open to the solvent. Moreover, the formation of the $(C)_1$ intermediate does not affect the conformation of the binding site. The lack of a strong increase of the MANT group fluorescence accompanying the formation of $(C)_1$ also suggests that the fluorophore has little contact with the hydrophobic areas of the binding site although it is strongly immobilized, as indicated by the strong increase of the MANT group fluorescence anisotropy (see below).

In the Second Intermediate the Bound Nucleotide Is Completely Isolated from the Solvent. The Stern−Volmer quenching constant, K_{SV_2}, for MANT-ATP and MANT-ADP in the second intermediate in the intrinsic nucleotide binding process, $(C)_2$, is 0.21 ± 0.1 and ~0, respectively. Such low, if any, quenching efficiency contrasts the behavior observed for the $(C)_1$ intermediate and indicates that in the $(C)_2$ intermediate the bound nucleotide is completely isolated from the solvent. Notice that the ribose moiety of the bound nucleotide is in contact with the binding site (see above). Thus, one possible explanation of these results could be that the transition $(C)_1 \leftrightarrow (C)_2$ results from the movement of the MANT group to a closed, hydrophobic pocket inside the nucleotide binding site. However, inspection of the rate constants characterizing the transition indicates that it is a very slow process (Tables 1 and 2, accompanying paper). Moreover, the process is energetically very unfavorable. This is rather surprising, if the transition results from interactions between the hydrophobic MANT moiety and a hydrophobic pocket in the binding site. Although, a simple placement of

the MANT group in a hydrophobic pocket cannot be excluded, it is very improbable that a movement of the small group would be such a slow and energetically unfavorable process. Rather, the obtained data suggest that the entire nucleotide-binding site of the DnaC protein changes its conformation and forms a state where the solvent is effectively excluded from accessing the bound nucleotide. A very strong increase of the MANT fluorescence accompanying the formation of the $(C)_2$ intermediate supports this conclusion.

Significant Immobilization of the Bound Nucleotide Already Occurs in the Formation of the First Intermediate $(C)_1$. Because the fluorescence intensity is strictly proportional to the concentration of a fluorophore, the time dependence of the emission intensity in a relaxation process is described by the same exponential functions as the concentrations of the reactants, with amplitudes weighted by the molar fluorescence intensities of all fluorescing species (*20*−*23*). Therefore, the correct mechanism of the reaction and relative molar fluorescence intensities, characterizing each individual intermediate of the reaction, can be determined by exclusively using the fluorescence emission (accompanying paper). As we pointed out above, relative molar intensities provide information about the physical environment of the fluorophore. On the other hand, the anisotropy provides a unique insight into the mobility of the bound ligand in each identified intermediate of the reaction.

Analysis of the time courses of anisotropy for MANT-ATP and MANT-ADP binding to the DnaC protein reveals a very intriguing result. The major mobility decrease of the MANT group occurs in the formation of the first intermediate $(C)_1$. This is despite the fact that the formation of $(C)_1$ is accompanied by large, positive entropy change (Table 5, see below). The observed anisotropy, r, increases from the value of $r \approx 0.015$, a characteristic of the free MANT-nucleotide in solution (14), to $r \approx 0.15$ in $(C)_1$ (Figure 6a,b). Subsequent transition to $(C)_2$ induces a moderate increase of r to $\sim$0.19.

The major decrease of the MANT mobility in $(C)_1$ occurs despite the fact that transient dynamic quenching studies indicate that the binding site in $(C)_1$ has an open conformation and the solvent has full access to the bound nucleotide (see above). Recall, adenine and the ribose are involved in very energetically favorable interactions with the binding site in $(C)_1$. These interactions are very specific, indicating that they include short-range bonds, e.g., hydrogen bonding. Thus, both base and ribose regions of the bound nucleotide are immobilized in the first intermediate. Moreover, the anisotropy of $\sim$0.015 for the free MANT-nucleotide in solution is larger than that predicted for the free rotating MANT moiety ($r \approx 0.0003$) (*18*, *14*, *21*). Therefore, these data strongly suggest significant stiffness of the covalent bond between the MANT group and the ribose, most probably resulting from the possible formation of the partial double-bond (*12*). In other words, the anisotropy of MANT-ATP and MANT-ADP reflects to a large extent the mobility of the entire nucleotide molecule in solution or in the binding site. A significant increase of the MANT group anisotropy in the first intermediate would simply reflect the fact that the MANT group is immobilized to a similar extent as the ribose region of the bound MANT-ATP or MANT-ADP. Transition to the $(C)_2$ intermediate closes the binding site leading to the diminished solvent accessibility and, possibly, the decreased mobility of the bound nucleotide through interactions with the hydrophobic areas of the binding site, as indicated by the large increase of the MANT fluorescence in $(C)_2$ (see above).

Salt Effect on the Nucleotide Binding Originates from the Formation of the First Intermediate $(C)_1$. Equilibrium studies clearly show that binding of MANT-ATP and MANT-ADP to the DnaC protein is accompanied by the net release of the $\sim$1 ion from the binding site (*11*). The analysis of the dynamics described in this work is in excellent agreement with the equilibrium data. Moreover, the kinetic data show that a single ion is released in the formation of the first intermediate, $(C)_1$, in the intrinsic nucleotide binding process. Notice that the formation of $(C)_1$ for MANT-ATP and MANT-ADP, differing by the number of the phosphate groups, is accompanied by the same number of ions released. This result provides support for the conclusion that the nucleotide binding process is predominantly initiated through adenine and ribose regions of the cofactor. However, the fact that both ATP and ADP analogues are characterized by the same affinity while the affinity of AMP (Galletto, unpublished data) is barely detectable indicates that the β-phosphate group may also participate in the stabilization of $(C)_1$ (*11*).

The lack of any salt effect on the $(C)_1 \leftrightarrow (C)_2$ transition in both MANT-ATP and MANT-ADP complexes with the DnaC protein indicates that closing the binding site and shielding the nucleotide from the solvent does not include a net ion release or uptake. Nevertheless, the increasing salt concentration in solution has a different effect on the structure of the $(C)_2$ intermediate formed by ATP and ADP analogues. While in the case of MANT-ADP the relative molar intensity of $(C)_2$ is not changed, the value of F_3 is higher at lower [NaCl] for MANT-ATP (Tables 3 and 4). Higher values of the F_3 observed for MANT-ATP than for the ADP analogue indicate that the ribose region of MANT-ATP is in a more hydrophobic environment, i.e., differently oriented in the $(C)_2$ intermediate than the ribose region of the ADP cofactor (accompanying paper). As the salt concentration decreases, the ribose region of MANT-ATP, but not MANT-ADP, is placed in an even more hydrophobic environment in the closed conformation of the $(C)_2$ intermediate.

The DnaC Conformational Transition Prior to the Nucleotide Binding Is Not Affected by the Salt in Solution. A very important aspect of the salt effect on the dynamics of the nucleotide binding to the DnaC protein is the discovery that the DnaC conformational transition, prior to MANT-ATP or MANT-ADP binding, is not affected by the salt in solution. The rate constants, k_1 and k_{-1}, and the resulting partial equilibrium constant, K_1, are affected very little by a 1 order of magnitude increase of the salt concentration. The same salt concentration change significantly affects the energetics and dynamics of the nucleotide binding (Tables 3 and 4) (*11*). In other words, binding of ions to the nucleotide-binding site does not affect the conformational transition of the protein prior to the nucleotide binding. Rather, the data indicate that the nucleotide binding and release exclusively control the equilibrium between the two conformations of the DnaC protein.

Formation of Different Intermediates in the Nucleotide Cofactor Binding to the DnaC Protein is Characterized by Very Different, Apparent Enthalpy and Entropy Changes. The temperature effect on partial equilibrium constants,

characterizing individual steps of the reaction, reveals large differences in the energetics of transitions between different intermediates. The pre-equilibrium conformational transition of the DnaC protein is apparently an enthalpy-driven process with an unfavorable entropy contribution. Favorable enthalpy and the lack of any net salt effect on this step strongly suggest that the process encompasses structural changes of the protein that do not include significant changes in the protein−solvent interactions. At present, it is not known whether the structural changes are global, i.e., whether they include large structural rearrangements of the protein or are local in nature and limited to the nucleotide-binding site. Our laboratory is currently studying these structural changes.

In the intrinsic nucleotide binding process, the formation of the first intermediate, $(C)_1$, is characterized by an unfavorable, positive enthalpy change and a large favorable entropy change (Table 5). The positive enthalpy change suggests that the cofactor binding imposes significant stress in the binding site that is overcome at the expense of a favorable entropy change. However, as we pointed out above, direct examination of the mobility of the nucleotide cofactors in the binding site, using fluorescence anisotropy, indicate that the mobility of the cofactor is strongly hindered in $(C)_1$ (Figure 6). Such limited mobility would suggest that an unfavorable entropy change should accompany the formation of $(C)_1$; however, this is not experimentally observed. Notice that the obtained entropy changes are apparent quantities that include all molecular events in the formation of $(C)_1$. Although the cofactor is being immobilized in the complex, the large observed positive entropy change strongly suggests that a significant number of solvents and/or solute molecules are released in the formation of $(C)_1$, although the solvent is still accessible to the bound nucleotide (see above). This conclusion is supported by the fact that, in this step, the net release of ~1 ion occurs and provides an additional positive contribution to the apparent positive entropy change (*29*).

Dynamic quenching of the transient intermediates indicates that in $(C)_2$ the nucleotide becomes shielded from the solvent (see above). The data indicate that the protein undergoes a structural transition resulting in a closed conformation of the nucleotide binding-site. A large negative enthalpy change accompanying the $(C)_1 \leftrightarrow (C)_2$ transition supports the conclusion that the transition includes protein conformational changes. Thus, these results strongly suggest that once the $(C)_1$ is formed the stress in the binding site can be released and the site and the cofactor assume an energetically more favorable orientation. However, the process is characterized by an apparent large negative entropy change (Table 5). This is despite the fact that the fluorescence anisotropy data indicate only moderate, additional immobilization of the cofactor in the binding site. In other words, the large entropy changes do not result from the immobilization of the bound cofactor but are most probably generated by the changes in the protein structure and/or its interactions with the solvent.

The discussed data also indicate an important caveat in the exclusive interpretation of thermodynamic or structural parameters in terms of the structure or nature of the formed complexes. Though large positive entropy changes would suggest significant mobility of the nucleotide in the $(C)_1$ intermediate, large negative entropy changes would suggest strong additional immobilization of the cofactor in $(C)_2$. On the other hand, direct fluorescence anisotropy studies indicate that this is not the case. The cofactor is strongly immobilized in $(C)_1$ and shows only a slight increase in the restriction of the movement in $(C)_2$. The entropy changes seem to be predominantly generated by the protein structural changes, and/or changes in the protein interactions with the solvent, accompanying the complex formation. Thus, a parallel application of the structural and thermodynamic analyses provides a deeper insight into the nature of the formed intermediates.

ACKNOWLEDGMENT

We wish to thank Gloria Drennan Bellard for her help in preparing the manuscript.

REFERENCES

1. Kornberg, A., and Baker, T. A. (1992) *DNA Replication*, Freeman, San Francisco.
2. Marians, K. J. (1992) *Annu. Rev. Biochem. 61*, 673−719.
3. Skarstad, K., and Wold, S. (1995) *Mol. Microbiol. 17*, 825−831.
4. Wickner, S., Wright, M., and Hurwitz, J. (1973) *Proc. Natl. Acad. Sci. U.S.A. 71*, 783−787.
5. Wickner, S., and Hurwitz, J. (1974) *Proc. Natl. Acad. Sci. U.S.A. 72*, 921−925.
6. Marians, K. J. (1999) *Prog. Nucl. Acid. Res. Mol. Biol. 63*, 39−67.
7. Wahle, E., Lasken, R. S., and Kornberg, A. (1989) *J. Biol. Chem. 264*, 2463−2468.
8. Wahle, E., Lasken, R. S., and Kornberg, A. (1989) *J. Biol. Chem. 264*, 2469−2475.
9. Allen, G. C., and Kornberg, A. (1991) *J. Biol. Chem. 266*, 22096−22101.
10. Allen, G. C., and Kornberg, A. (1991) *J. Biol. Chem. 268*, 19204−19209.
11. Galletto, R., Rajendran, S., and Bujalowski, W. (2000) *Biochemistry 39*, 12959−12969.
12. Hiratsuka, T. (1983) *Biochim. Biophys. Acta 742*, 496−508.
13. Bujalowski, W., and Klonowska, M. M. (1993) *Biochemistry 32*, 5888−5900.
14. Bujalowski, W., and Klonowska, M. M. (1994) *Biochemistry 33*, 4682−4694.
15. Bujalowski, W., and Klonowska, M. M. (1994) *J. Biol. Chem. 269*, 31359−31371.
16. Jezewska, M., J., Kim, U.-S., and Bujalowski, W. (1997) *Biophys. J. 71*, 2075−2086.
17. Eftink, M. R., and Ghiron, C. A. (1981) *Anal. Biochem. 114*, 199−227.
18. Lakowicz, J. R. (1999) *Principle of Fluorescence Spectroscopy*, Plenum Press, New York.
19. Jezewska, M. J., and Bujalowski, W. (1997) *Biophys. Chem. 64*, 253−269.
20. Bujalowski, W., and Jezewska, M. J. (2000) *J. Mol. Biol. 295*, 831−852.
21. Bujalowski, W., and Jezewska, M. J. (2000) *Biochemistry 39*, 2106−2122.
22. Rajendran, S., Jezewska, M. J., and Bujalowski, W. (2001) *Biochemistry 40*, 11794−11810.
23. Jezewska, M. J., Rajendran, S., and Bujalowski, W. (2001) *J. Mol. Biol. 313*, 977−1002.
24. Jezewska, M. J., Rajendran, S., and Bujalowski, W. (1998) *Biochemistry 37*, 3116−3136.
25. Bujalowski, W., and Jezewska, M. J. (2000) in *Spectrophotometry & Spectrofluorimetry. A Practical Approach* (Gore, M. G., Ed.) Chapter 5, Oxford University Press, New York.
26. Bernasconi, C. J. (1976) *Relaxation Kinetics*, Academic Press, New York.
27. Otto, R., Lillo, M. P., and Beechem, J. M. (1994) *Biophys. J. 67*, 2511−2521.
28. Pilar, R. L. (1968) *Elementary Quantum Chemistry*, Chapter 9, McGraw-Hill, New York.
29. Record, M. T., Jr., Anderson, C. F., and Lohman, T. M. (1978) *Q. Rev. Biophys. 11*, 103−178

BI020127W